Arsenic trioxide potentiates the effectiveness of etoposide in Ewing sarcomas

KAREN A. BOEHME[1*], JULIANE NITSCH[1*], ROSA RIESTER[1], RUPERT HANDGRETINGER[2], SABINE B. SCHLEICHER[2], TORSTEN KLUBA[3,4] and FRANK TRAUB[1,3]

[1]Laboratory of Cell Biology, Department of Orthopaedic Surgery, Eberhard Karls University Tuebingen;
[2]Department of Haematology and Oncology, Children's Hospital, Eberhard Karls University Tuebingen;
[3]Department of Orthopaedic Surgery, Eberhard Karls University Tuebingen, Tuebingen;
[4]Department for Orthopaedic Surgery, Hospital Dresden-Friedrichstadt, Dresden, Germany

Abstract. Ewing sarcomas (ES) are rare mesenchymal tumours, most commonly diagnosed in children and adolescents. Arsenic trioxide (ATO) has been shown to efficiently and selectively target leukaemic blasts as well as solid tumour cells. Since multidrug resistance often occurs in recurrent and metastatic ES, we tested potential additive effects of ATO in combination with the cytostatic drugs etoposide and doxorubicin. The Ewing sarcoma cell lines A673, RD-ES and SK-N-MC as well as mesenchymal stem cells (MSC) for control were treated with ATO, etoposide and doxorubicin in single and combined application. Viability and proliferation (MTS assay, colony formation, 3D spheroid culture) as well as cell death induction (western blot analysis, flow cytometry) were analysed. In the MTS viability assays ATO treatment significantly reduced the metabolic activity of all three ES cell lines (A673, RD-ES and SK-N-MC) examined. Moreover, all ES cell lines were sensitive to etoposide, whereas MSC remained unaffected by the drug concentrations used. With the exception of ATO in RD-ES cells, all drugs induced apoptosis in the ES cell lines, indicated by caspase-3 and PARP cleavage. Combination of the agents potentiated the reduction of viability as well as the inhibitory effect on clonal growth. In addition, cell death induction was obviously enhanced in RD-ES and SK-N-MC cells by a combination of ATO and etoposide compared to single application. Summarised, the combination of low dose, physiologically easily tolerable ATO with commonly used etoposide and doxorubicin concentrations efficiently and selectively suppressed viability and colony formation in ES cell lines, whereas a combination of ATO and etoposide was favourable for cell death induction. In addition to an increase of the effectiveness of the cytostatic drugs and prevention of potential drug resistance, this approach may also reduce toxicity effects, since the individual doses can be reduced.

Correspondence to: Dr Karen A. Boehme, Laboratory of Cell Biology, Department of Orthopaedic Surgery, Eberhard Karls University Tuebingen, Waldhoernlestrasse 22, D-72072 Tuebingen, Germany
E-mail: karen.boehme@web.de

Introduction

Ewing sarcomas (ES) are rare, aggressive mesenchymal tumours affecting bones and soft tissues with a peak incidence in childhood and adolescence (1). In ~85% of patients a t(11;22) (q24;q12) chromosomal translocation can be detected leading to expression of a chimeric fusion protein composed of the *Ewing sarcoma breakpoint region 1 (EWS)* gene on chromosome 22 and the *Fried leukaemia integration 1 (FLI1)* gene on chromosome 11. Moreover, other less common fusion proteins have been described mostly comprising the EWS transactivation domain (2). The aberrant transcription factor EWS-FLI1 activates several signalling pathways promoting proliferation and apoptosis resistance (3-5).

The standard of care for ES is a neo-adjuvant chemotherapy including doxorubicin, vincristine, cyclophosphamide, actinomycin D, ifosfamide and etoposide followed by surgery, conceivably radiation therapy and adjuvant chemotherapy (6,7). Five-year survival rates for localised disease are ~70%. However, patients with metastases expect only 5-year survival rates of 20-30% (1).

Multidrug resistance is a common problem in metastatic and recurrent ES and increases during prolonged therapy (8). Multidrug resistance associated protein 1 (MRP1) overexpres-

sion is a common feature of ES, whereas multidrug resistance protein 1 (MDR1) expression is less common (9). Substrate specificity of both ABC transporters includes etoposide, doxorubicin and vincristine implicating their role in therapeutic resistance of ES (10).

Several clinical trials specifically targeting receptor tyrosine kinases such as insulin-like growth factor receptor 1 (IGF-1R), kit, platelet-derived growth factor receptor (PDGFR), epidermal growth factor receptor (EGFR), vascular growth factor receptor (VEGFR) or other proteins including Aurora kinase A, mammalian target of rapamycin (mTOR) or poly (ADP-ribose) polymerase 1 (PARP1) in ES family tumours are currently in phase I and II. However, response rates in ES are usually <30% (1). Combination therapy using cytotoxic drugs and targeted therapeutics may be an opportunity to overcome drug resistance and improve survival.

The glioma associated oncogene family 1 (GLI1) transcription factor is a direct transcriptional target of the EWS-FLI1 fusion protein (11-13). In several types of cancer, including ES and rhabdomyosarcoma (RMS), GLI1 has been associated with proliferation and survival (12,14). Targeting GLI by arsenic trioxide (ATO) has been shown to reduce viability of several ES cell lines with an IC_{50} of ~1 μM using a WST-1 viability assay (15). Additionally, ATO inhibits migration and invasion capacity of RD-ES and A673 cells (16). Moreover, Matsumoto *et al* reported that GANT61, another GLI inhibitor, was capable of inducing caspase-3 and -7 independent cell death in the ES cell line SK-N-LO (17).

In this study, we determined whether GLI inhibition using ATO or GANT61 specifically and efficiently compromises three different ES cell lines compared to mesenchymal stem cells (MSC). Based on our results, we selected ATO for combination experiments with etoposide and doxorubicin. Especially, the combination of ATO and etoposide significantly exceeded the effect of each single drug on viability reduction, clonal growth and cell death induction in ES cell lines, whereas MSC were hardly compromised by the drug doses applied in the experiments.

Materials and methods

Reagents. ATO (Trisenox, Pharmacy of University Hospital Tuebingen) was dissolved in purified water, GANT61 (Abcam, Cambridge, UK), etoposide and doxorubicin (Selleckchem, Munich, Germany) were dissolved in dimethyl sulfoxide. For cell culture treatment stock solutions were further diluted in culture medium.

Cell lines and culture. RD-ES and A673 cells were obtained from CLS Cell Lines Service GmbH (Eppelheim, Germany). SK-N-MC were purchased from ATCC (Manassas, VA, USA). RD-ES and SK-N-MC cells were maintained in RPMI-1640 with L-glutamine (Gibco, Life Technologies, Darmstadt, Germany) supplemented with 15% FCS (Biochrom, Berlin, Germany). A673 cells were cultivated in Dulbecco's modified Eagle's medium with GlutaMAX, 4.5 g/l D-glucose (Gibco, Life Technologies) supplemented with 10% FCS (Biochrom). Bone marrow derived MSC were isolated at the University Hospital Tuebingen after written informed consent of the patients (approved by The Ethics Committee of the Medical

Faculty, project no. 401/2013 BO_2), propagated as described before (18) and confirmed to represent multi-lineage differentiation potential toward chondrocytes, adipocytes and osteocytes (data not shown). All cells were cultivated at 37°C in humidified atmosphere containing 5% CO_2.

RNA isolation and qRT-PCR. RNA was isolated using the innuPREP RNA Mini kit (Analytik Jena AG, Jena, Germany). RNA (1 μg) was reverse transcribed using the innuSCRIPT reverse transcriptase (Analytik Jena AG). cDNA (50 ng) was analysed in duplicate reactions by quantitative RT-PCR (qRT-PCR) using gene-specific primers and the SYBR Select Master mix for CFX (Life Technologies GmbH) in a total volume of 10 μl. qRT-PCR was carried out in a CFX96 real-time device (Bio-Rad, Munich, Germany) and was analysed using the CFX Manager™ software (Bio-Rad). Relative expression levels were calculated as fold change compared to MSC using the $\Delta\Delta Ct$ ($2^{-\Delta\Delta Ct}$) method with TATA box binding protein (TBP) as a reference gene. Hh pathway primers were used according to Laurendeau *et al* (19).

Cytotoxicity assay. Cell Titer 96® AQueous One Solution Cell Proliferation (MTS) assay (Promega, Mannheim, Germany) was used to measure cell viability via redox enzyme activity, according to the protocol provided by the manufacturer. A673, RD-ES, SK-N-MC and MSC (0.5-1x10^4 cells/well) were grown in 96-well plates. Twenty-four hours after seeding, the cells were incubated in the presence of ATO, GANT61, etoposide, doxorubicin or inhibitor combinations for another 96 h at 37°C in a humidified atmosphere of 5% CO_2 in air. At the end of the incubation period, MTS reagent was added to the wells, and the plate was incubated for 1.5 h protected from light. Absorbance was recorded at 490 nm with a reference wavelength of 630 nm using an EL 800 reader (BioTek, Winooski, VT, USA).

IC_{50} determination. IC_{50} values of ATO, GANT61, etoposide and doxorubicin were determined for the different cell lines by non-linear regression using GraphPad Prism V6.0 software.

Colony formation assay. A673 cells were plated at a density of 1x10^3 cells/well, RD-ES cells were plated at a density of 0.5x10^3 cells/well and SK-N-MC were plated at a density of 1.5x10^3 cells/well in a 6-well plate and incubated with increasing concentrations of ATO, etoposide, doxorubicin or inhibitor combinations for 72 h, followed by substitution of the culture medium. After 10 days subsequent growth in standard growth medium, cells were fixed using ice cold methanol for 10 min, washed and stored in PBS. Visualisation of fixed cell colonies was achieved by incubating the cells with 0.5% (w/v) crystal violet for 30 min. Excess crystal violet was removed by washing with ddH$_2$O. Visible colonies consisting of ≥50 cells were counted. The colony formation rate was determined: (number of colonies/number of plated cells) x 100.

Spheroid assay. For generation of 3D spheroids 0.5x10^4 cells of the ES cell line A673 or 0.25x10^4 cells of the ES cell line SK-N-MC were seeded in ultra-low-attachment, U-bottom 96-well plates (Thermo Scientific, Rochester, NY, USA). After 96 h spheroid formation was documented by micrographs and

ATO, etoposide and doxorubicin were added to the culture medium as indicated. Ninety-six hours later a second documentation by micrographs was performed.

Western blot analysis. A673, RD-ES, SK-N-MC or MSC (2.5×10^5 each) were incubated in 12-well plates with inhibitor concentrations indicated for 48 h. For analysis, cells were washed with PBS and lysed in protein lysis buffer (40 mM Tris/HCl pH 7.4, 300 mM NaCl, 2 mM EDTA, 20% glycerol, 2% Triton X-100) supplemented with proteinase inhibitor at 4°C. Insoluble material was removed by centrifugation. The protein concentration in the supernatant was determined by Bradford protein assay. Protein samples (40 μg) were separated by 10% SDS-PAGE and transferred to a hydrophobic polyvinylidene difluoride (PVDF) membrane (Immobilon-P; Merck KGaA, Darmstadt, Germany). After blocking with 5% powdered milk (Carl Roth, Karlsruhe, Germany) in TBS-T, membranes were incubated with primary antibodies [GLI1 rabbit pAb #2553, β-tubulin (9F3) rabbit mAb #2128, cleaved caspase-3 (5A1E) rabbit mAb #9664, anti-cleaved PARP (DE64E10) rabbit mAb #5625, all 1:1,000, Cell Signaling Technology, Leiden, The Netherlands; GLI2 (H300) rabbit pAb, 1:200, sc-28674, Santa Cruz Biotechnology Inc., Dallas, TX, USA] with gentle shaking overnight at 4°C according to the manufacturer's protocols. Membranes were washed three times with TBS-T. Secondary antibody (horseradish peroxidase-conjugated anti-rabbit pAb, 1:10,000, Jackson Immuno Research, West Grove, PA, USA) was added for 2 h, and the membranes were washed another three times with TBS-T. Proteins were detected using ECL Western Blotting Substrate (Thermo Scientific, Waltham, MA, USA) with membranes exposed to Amersham Hyperfilm ECL (GE Healthcare, Pittsburgh, PA, USA). A pre-stained protein ladder (PageRuler Plus, Thermo-Scientific) was used for determination of molecular weights. ImageJ (NIH) was utilised for western blot quantification.

Flow cytometry. Cell membrane integrity as indicator for cell death was determined using the fixable viability dye eFluor® 450 (eBioscience, San Diego, CA, USA). A673 (2.5×10^5), RD-ES (1.5×10^5), SK-N-MC (1×10^5) or MSC (2.5×10^5) were incubated with inhibitor concentrations indicated for 72 h, washed with PBS, detached with trypsin, and stained for 30 min at 4°C in the dark. Cells were washed with PBS and fixed with 0.5% formaldehyde diluted in PBS before being resuspended in FACS buffer (PBS containing 2% FCS, 2 mM EDTA). Flow cytometric analysis was performed on an LSRII flow cytometer (Becton-Dickinson, Franklin Lakes, NJ, USA) using FlowJo Software (Tree Star Inc., Ashland, OR, USA) for data evaluation.

Statistical analysis. All statistical tests were performed using GraphPad Prism V6.0 software and statistical differences were analysed by two-way ANOVA with $p \leq 0.05$, $p \leq 0.01$ and $p \leq 0.001$ considered as statistically significant. Multiple comparisons between groups were performed using Tukey's test.

Results

Expression of hedgehog pathway genes in ES cell lines. Hh pathway gene expression was determined in three human ES cell lines, compared to MSC (Fig. 1A). Quantitative real-time

Table I. Hh pathway inhibition and cytostatic drugs reduce viability in human ES cell lines.

Inhibitor	Cell line	IC$_{50}$
ATO	MSC	>10.00 μM
	A673	0.23 μM
	RD-ES	1.91 μM
	SK-N-MC	4.42 μM
GANT61	MSC	16.05 μM
	A673	12.01 μM
	RD-ES	35.37 μM
	SK-N-MC	59.56 μM
Etoposide	MSC	>35.00 μM
	A673	0.88 μM
	RD-ES	1.06 μM
	SK-N-MC	1.11 μM
Doxorubicin	MSC	>150.00 nM
	A673	27.18 nM
	RD-ES	115.00 nM
	SK-N-MC	75.15 nM

MTS assays were performed four days after treatment with ATO, GANT61, etoposide or doxorubicin in three ES cell lines and mesenchymal stem cells (MSC) in quadruplicate. Mock-treated control was set to 100% viability. IC$_{50}$ values were determined by non-linear regression of MTS results using GraphPad Prism 6.

PCR revealed that GLI1 mRNA expression was considerably elevated in A673 cells compared to MSC, whereas it was downregulated in SK-N-MC. Also GLI2 mRNA was slightly overexpressed in A673, whereas its expression level in RD-ES and SK-N-MC resembled the MSC control. GLI3 mRNA was marginally overexpressed in A673, but downregulated in RD-ES and SK-N-MC. SMO mRNA expression was slightly enhanced in A673 and SK-N-MC compared to MSC, whereas it was downregulated in RD-ES. Hh receptor PTCH1 mRNA was overexpressed in all ES cell lines compared to MSC, however only A673 cells showed a strong overexpression.

GLI1 protein expression was analysed by western blotting in ES cell lines and MSC (Fig. 1B). All splice variants ≥100 kDa were quantified and normalised to tubulin expression. The graph shows the full length GLI1 protein expression relative to MSC. In contrast to the overexpression of GLI1 mRNA, GLI1 protein expression of A673 cells mostly resembled MSC. In RD-ES and SK-N-MC GLI1 protein expression was reduced compared to MSC. In addition, GLI2 protein expression was determined by western blotting. The abundance of the full length and repressor form was quantified and normalised to tubulin expression. Both, GLI2 full length and repressor protein was expressed in all ES cell lines, however being very faint compared to the expression in MSC (Fig. 1C).

GLI inhibition and cytotoxic drugs reduce viability of human ES cell lines. MTS viability assays were performed to determine IC$_{50}$ values of ATO, GANT61, etoposide and doxorubicin in the three ES cell lines and MSC (Table I). While viability
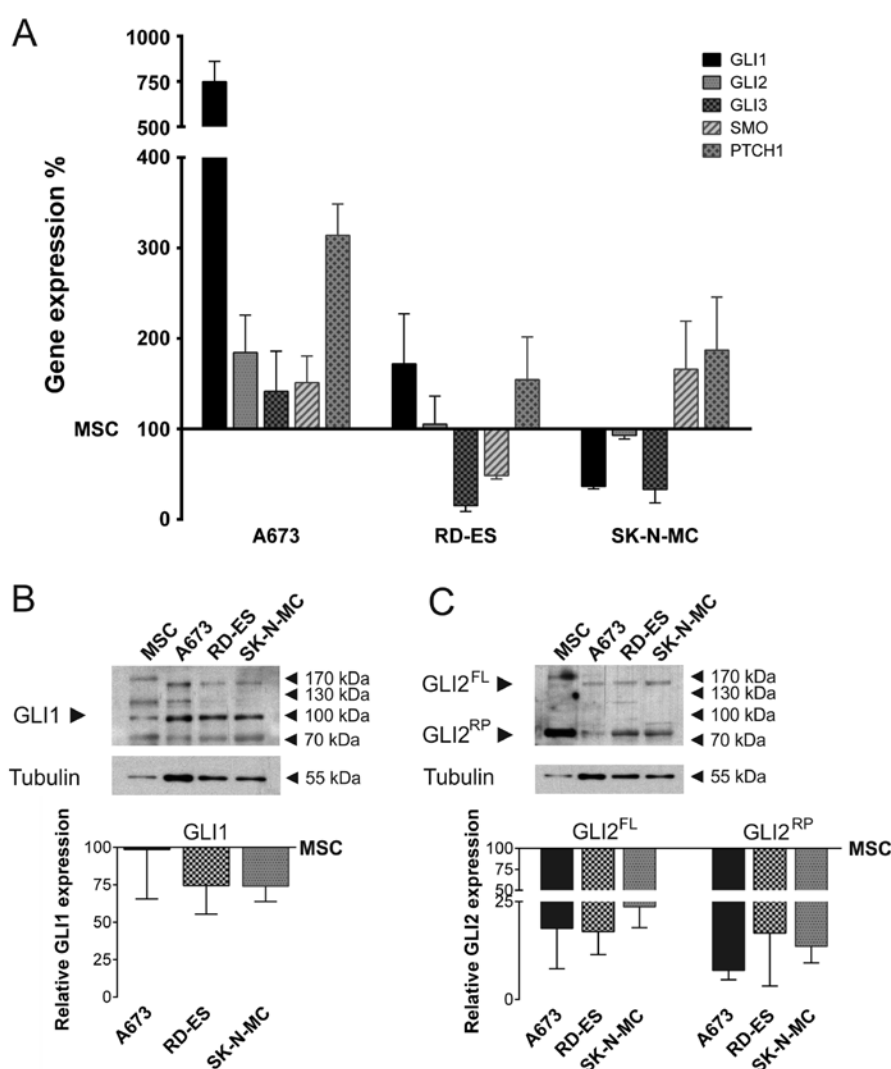
Figure 1. Human ES cell lines express Hh pathway genes. (A) Total RNA was extracted from three ES cell lines and MSC. Quantitative RT-PCR was performed for the genes GLI1, GLI2, GLI3, SMO and PTCH1 in quadruplicate and normalised to the housekeeping gene TBP. Expression levels relative to human MSC are shown. (B and C) Protein was extracted from three ES cell lines and MSC and western blot analysis was performed for GLI1 (B) or GLI2 (C) expression, tubulin was used as loading control. Signals of three independent experiments were quantified. The graphs show the mean values and standard deviations of GLI1 full length protein (B) or GLI2 full length (GLI2^{FL}) and repressor (GLI2^{RP}) protein expression (C) compared to MSC.

of MSC was still 82.4% after 96 h of incubation with 10 μM ATO, the IC$_{50}$ values for the ES cell lines ranged from 0.23 μM in A673 to 4.42 μM in SK-N-MC. This indicates that ATO specifically reduced viability of the tumour cell lines using doses ≤5 μM. The second GLI inhibitor, GANT61, inhibited the viability of A673 cells with an IC$_{50}$ of 12.01 μM. A similar IC$_{50}$ of 16.05 μM was obtained in MSC. In contrast, both RD-ES (IC$_{50}$ 35.37 μM) and SK-N-MC (IC$_{50}$ 59.56 μM) were significantly more resistant to GANT61. Using 35 μM of the topoisomerase inhibitor etoposide 85.6% of MSC were viable. In contrast, the IC$_{50}$ values obtained in the ES cell lines were 0.88 μM (A673), 1.06 μM (RD-ES) and 1.11 μM (SK-N-MC) revealing a high sensitivity. Doxorubicin, a DNA intercalating anthracycline, reduced the viability of A673 cells with an IC$_{50}$ of 27.18 nM. SK-N-MC (IC$_{50}$ 75.15 nM) and RD-ES (IC$_{50}$ 115 nM) were more resistant. MSC (58.6±1%) were still viable at the highest doxorubicin dose used (150 nM), recommending the use of lower doxorubicin doses to specifically target the tumour cells.

Combination of ATO with etoposide and doxorubicin augments viability reduction. To determine potential additive effects of ATO and the cytostatic agents etoposide and doxorubicin, low doses of ATO and both chemotherapeutics were used in combination experiments. The individual concentrations were adjusted for each cell line to consider specific sensitivities for each substance (Fig. 2). A673 cells showed a significant viability reduction to 40.1±4.9% compared to mock-treated control after the combination of 0.1 μM ATO and 1 μM etoposide, whereas additional application of 5 nM doxorubicin reduced viability to 32.8±1.3%. After the double treatment with the respective ATO and doxorubicin doses viability was hardly affected, while the single application of 1 μM etoposide was sufficient to reduce the metabolic activity of A673 cells to 63.1±5.1%. Due to the very distinct sensitivity of the A673 cell metabolism to ATO, combination experiments were performed with extremely low ATO concentrations. The etoposide dose applied for these cells corresponded to the half maximal inhibitory concentration. In RD-ES cells a combina-
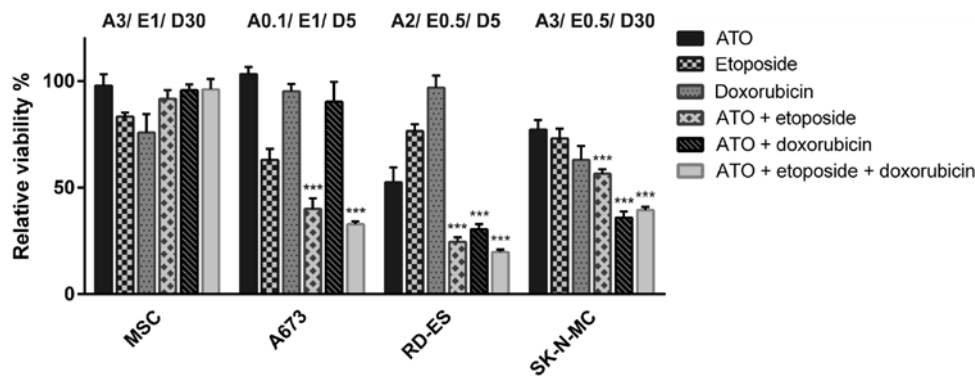
Figure 2. ATO in combination with cytostatic drugs enhances viability reduction in human ES cell lines. MTS assays were performed four days after single or combined treatment of three ES cell lines and MSC with ATO, etoposide and doxorubicin in quadruplicate. Mock-treated control was set to 100% viability (A, μM ATO; E, μM etoposide; D, nM doxorubicin). Error bars indicate the standard deviations (***p≤0.001 relative to single treatment).
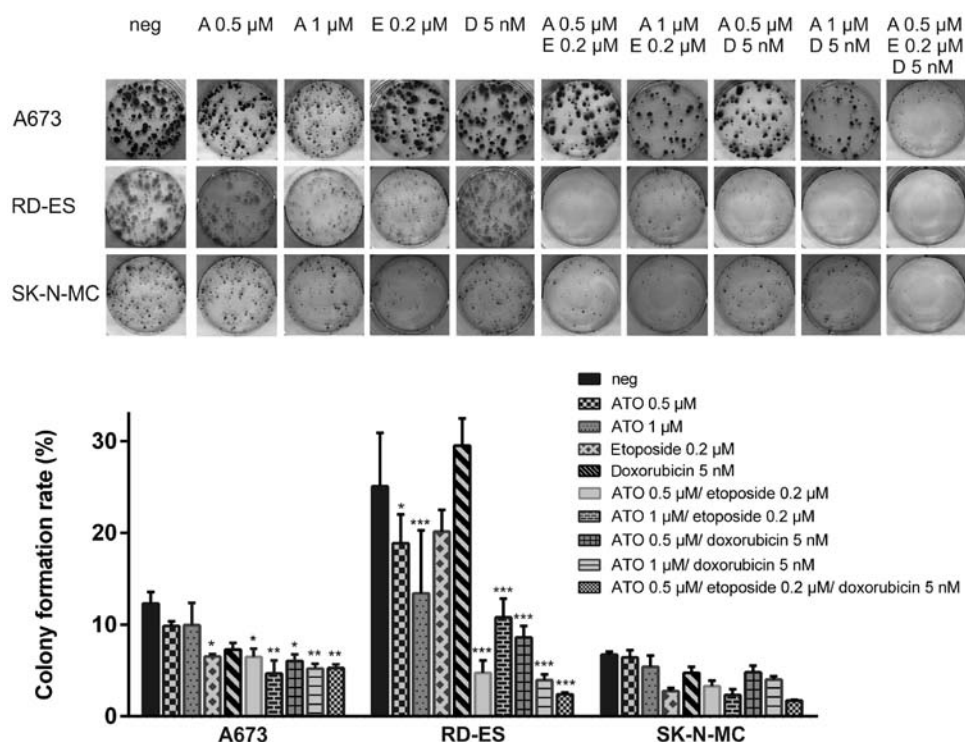

Figure 3. ATO in combination with etoposide or doxorubicin impairs colony formation of ES cell lines. A673 cells (1×10^3), 0.5×10^3 RD-ES or 1.5×10^3 SK-N-MC cells were seeded in 6-well plates and incubated with the ATO (A), etoposide (E) or doxorubicin (D) concentrations indicated for 72 h. Subsequently, cells were incubated in normal culture medium for another ten days. Visualisation of fixed cell colonies was achieved by incubating the cells with 0.5% (w/v) crystal violet. Representative images for each cell line are shown. Colonies of three independent experiments were counted. The graph indicates the mean colony formation rates with standard deviations (*p≤0.05, **p≤0.01, ***p≤0.001 relative to mock-treated control).

tion of 2 μM ATO and 0.5 μM etoposide or 5 nM doxorubicin reduced the viability <30% of mock-treated control, which was only slightly enhanced by the triple combination (19.8±1.1%). Regarding the single drug applications used, the dose of 2 μM ATO was most efficient (52.5±7%) in RD-ES cells, representing the half maximal inhibitory concentration. With the exception of etoposide, SK-N-MC cells were more resistant to the single drugs compared to the other ES cell lines. Best results for combination treatment were achieved after incubation with 3 μM ATO and 30 nM doxorubicin (35.8±3.1% viable cells). The combination of 3 μM ATO with 0.5 μM etoposide was less effective (56.6±2.1% viable cells) and also the triple combination did not exceed the combined ATO and doxorubicin effect

(39.5±1.5%). MSC were not severely affected by the highest substance doses of 3 μM ATO, 1 μM etoposide and 30 nM doxorubicin used for the ES cells. Indeed, viability was still higher after treatment with drug combinations compared to the applied etoposide (83.39±1.9% viable cells) and doxorubicin (75.84±8.7% viable cells) concentrations alone.

ATO in combination with etoposide and doxorubicin impairs colony formation of ES cell lines. Colony formation assays were performed in the ES cell lines A673, RD-ES and SK-N-MC using 0.5 μM or 1 μM ATO in combination with 0.2 μM etoposide or 5 nM doxorubicin (Fig. 3). The colony formation rate of mock-treated RD-ES cells (25.1±5.8%) was higher
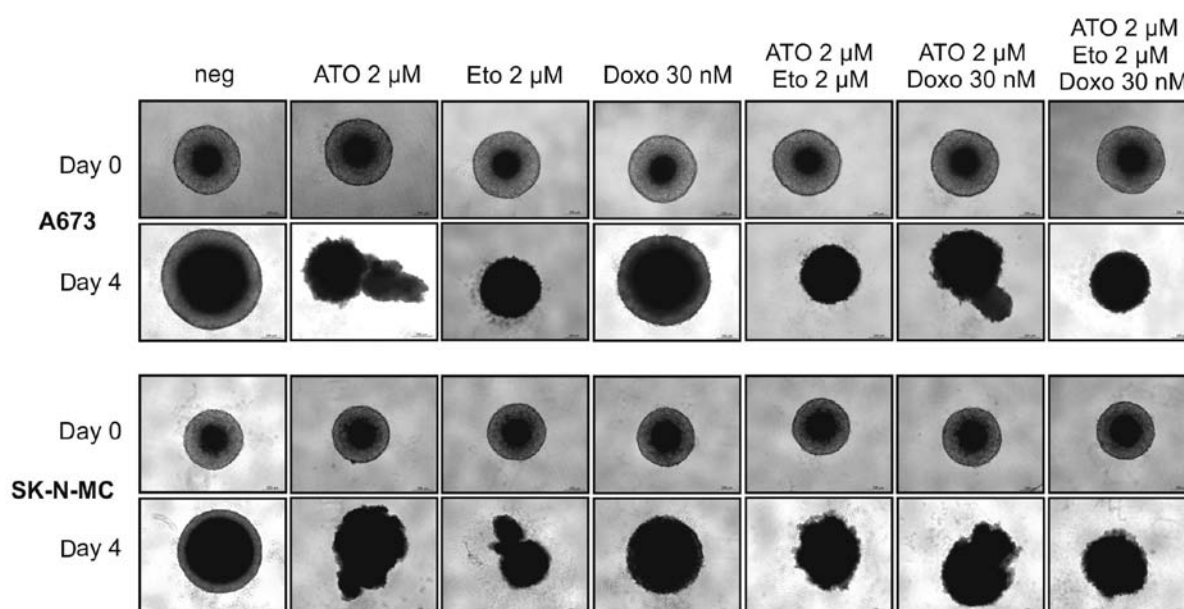
Figure 4. ATO, etoposide, doxorubicin and drug combinations reduce ES cell growth of 3D spheroid cultures. A673 (0.5×10^4) or 0.25×10^4 SK-N-MC cells were plated in non-adherent, U-bottom 96-well plates. After four days spheroid formation was documented with the microscope (day 0). Spheroids were incubated with the ATO, etoposide (Eto) and doxorubicin (Doxo) concentrations indicated for another four days whereupon a second micrograph was taken (day 4). Representative micrographs of three independent experiments are shown.

compared to A673 (12.3±1.3%) or even SK-N-MC, where only 6.7±0.3% of the plated cells formed colonies. Single application of 0.2 μM etoposide significantly reduced colony numbers in A673 cells (6.5±0.3%) and the combination of 0.2 μM etoposide and 1 μM ATO exceeded the effect of the single treatment (colony formation rate 4.7±1.4%). Also combination of 5 nM doxorubicin with 1 μM ATO (5.2±0.5% remaining colonies) was superior compared to the single agents in A673. The triple combination using 0.5 μM ATO, 0.2 μM etoposide and 5 nM doxorubicin was equally efficient compared to both double treatments utilising 1 μM ATO. Interestingly, just A673 cells, being extremely ATO sensitive in the viability assays, were quite resistant in these experiments with several small colonies remaining even after the triple treatment.

In RD-ES cells, ATO single treatment was already sufficient to significantly reduce colony formation (colony formation rate 0.5 μM ATO: 9.9±0.5%, 1 μM ATO: 9.9±2.4%), whereas 0.2 μM etoposide or 5 nM doxorubicin had less impact. Combination of both ATO concentrations with etoposide or doxorubicin potentiated the decline of colony formation with the combination of 5 nM doxorubicin and 1 μM ATO (colony formation rate 3.9±0.6%) being the most efficient. The triple combination was still superior to all double combinations reducing the colony formation rate to 2.4±0.2%.

Due to generally restricted colony formation of SK-N-MC cells no treatment led to a significant reduction of colony numbers counted. However, etoposide as well as the combination of 1 μM ATO and 0.2 μM etoposide reduced the colony formation rate <3%, whereas the triple combination was the most efficient (1.7±0.1% residual colonies).

Etoposide, ATO and combinations thereof reduce ES cell growth in 3D spheroid cultures. To simulate gradients in nutrition and oxygen availability as well as drug penetration

in vivo we used 3D spheroid cultures of A673 and SK-N-MC cells (Fig. 4). The cell line RD-ES refused to form stable 3D cultures and had to be excluded from this experiment. Drug concentrations used in single, double and triple application in this assay were 2 μM ATO, 2 μM etoposide and 30 nM doxorubicin. Especially 2 μM etoposide reduced the spheroid size and cohesion after four days of incubation in both ES cell lines. ATO (2 μM) also partially lysed the spheroids, whereas 30 nM doxorubicin were less efficient compared to the other agents. For both, A673 and SK-N-MC cells, none of the combinations outranked the effect of etoposide single treatment.

ATO, etoposide and doxorubicin induce cell death in ES cell lines. To exclude that the drugs have only transient growth arresting and viability reducing properties, flow cytometry analysis to detect incorporation of the fixable viability dye eFluor® 450 was performed. The dye is excluded from cells with intact membranes, therefore apoptotic or necrotic cells with membrane degradation can be quantified using this method. The ES cell lines A673, RD-ES and SK-N-MC as well as MSC were incubated with ATO, GANT61, etoposide or doxorubicin for three days (Fig. 5). ATO (5 μM) was sufficient to induce maximum cell death compared to the other treatments in this assay. Indeed, within the ES cell lines RD-ES exhibited the lowest amount of dead cells (41±2.7%) after incubation with 5 μM ATO, whereas 70±1.9% of SK-N-MC and 68±3.6 of A673 cells lost membrane integrity three days after application of this dose. GANT61, on the other hand, failed to induce significant cell death in all three ES cell lines at the concentration of 15 μM. Also treatment with 5 μM etoposide was sufficient to induce significant death rates in A673 cells (65.2±2.4%). The response of RD-ES cells was much less distinct (19.9±3.8%), while SK-N-MC exhibited an intermediate death rate of 38.5±7.4% compared to mock-treated
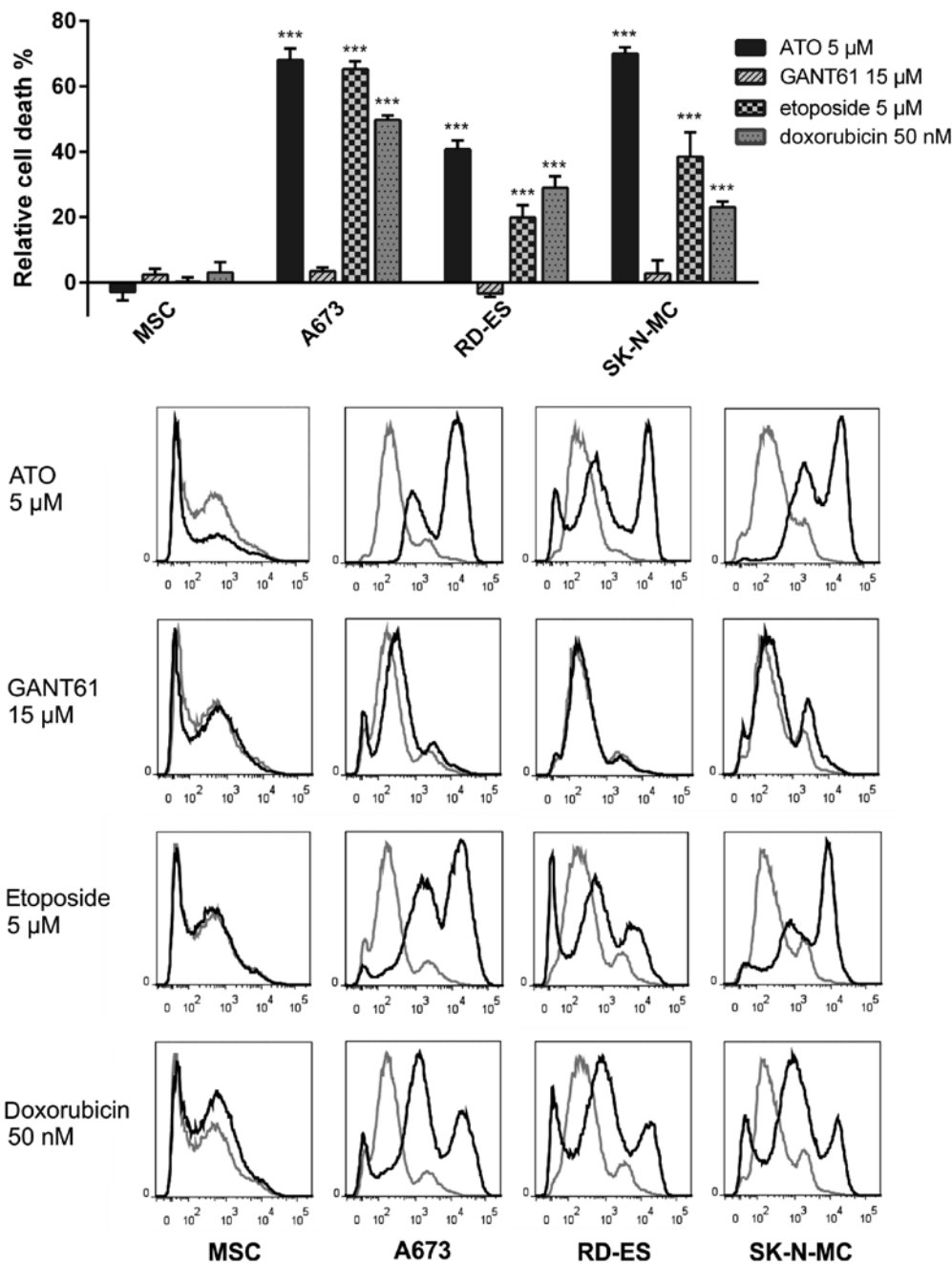
Figure 5. ATO, etoposide and doxorubicin induce cell death in human ES cell lines. Incorporation of the fixable viability dye eFluor® 450 was analysed by flow cytometry three days after treatment with ATO, GANT61, etoposide or doxorubicin in three ES cell lines and MSC in triplicate. Mock-treated control was set to 0% cell death. Error bars indicate the standard deviations (***p≤0.001 relative to MSC cell death). For all treatments (black curves) and corresponding mock-treated controls (grey curves) representative FACS histogram plots are shown.

control. As for the other substances, the death rate after incubation with 50 nM doxorubicin obtained in A673 cells was higher (49.7±1.4%) than in RD-ES (28.9±3.6%) or SK-N-MC (23±1.7%). For MSC no significant cell death induction was detectable using any of the substances.

Combination of ATO and etoposide potentiates the cell death induction in ES cell lines. In combination experiments detecting incorporation of the fixable viability dye eFluor® 450 (Fig. 6) ATO, etoposide and doxorubicin concentrations were used according to the MTS approach. In A673 cells 1 μM etoposide was sufficient to induce 49.1±1.2% cell death,

which was, in contrast to the viability assay, not exceeded by the combination with 0.1 μM ATO (50.6±4.4%) or the triple combination including 5 nM doxorubicin (52.5±2.8%). Membrane integrity was not affected by the low ATO and doxorubicin concentrations applied. In RD-ES cells, both the combination of 2 μM ATO and 0.5 μM etoposide as well as the triple combination including 5 nM doxorubicin clearly surpassed the efficiency of each single substance. However, the death rate after application of the triple combination (45.7±1.4%) was not higher compared to the double treatment using ATO and etoposide (49.2±2.7%). The ATO-doxorubicin combination showed a comparable impact (32.6±0.8% dead
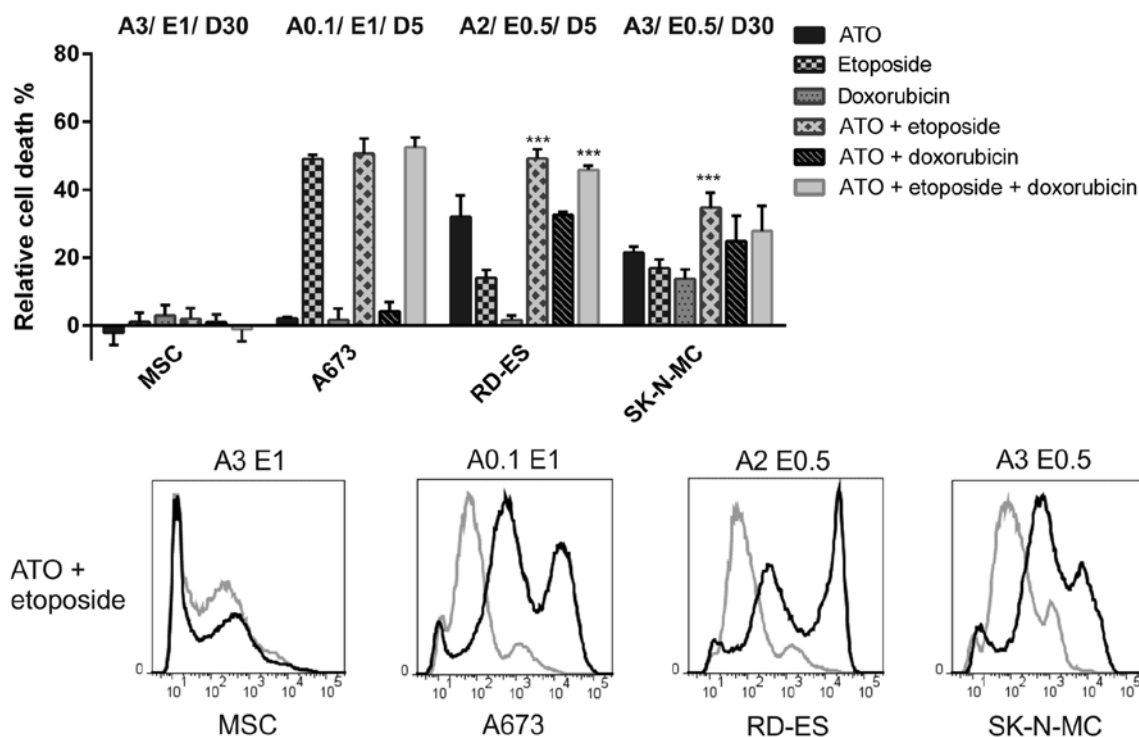
Figure 6. ATO in combination with etoposide enhances cell death induction in human ES cell lines. Incorporation of the fixable viability dye eFluor® 450 was analysed by flow cytometry three days after single or combined treatment with ATO, etoposide and doxorubicin in three ES cell lines and MSC in triplicate. Mock-treated control was set to 0% cell death. Error bars indicate the standard deviations (***p≤0.001 relative to single treatment). For combined treatment with ATO and etoposide (black curves) and corresponding mock-treated controls (grey curves) representative FACS histogram plots are shown.
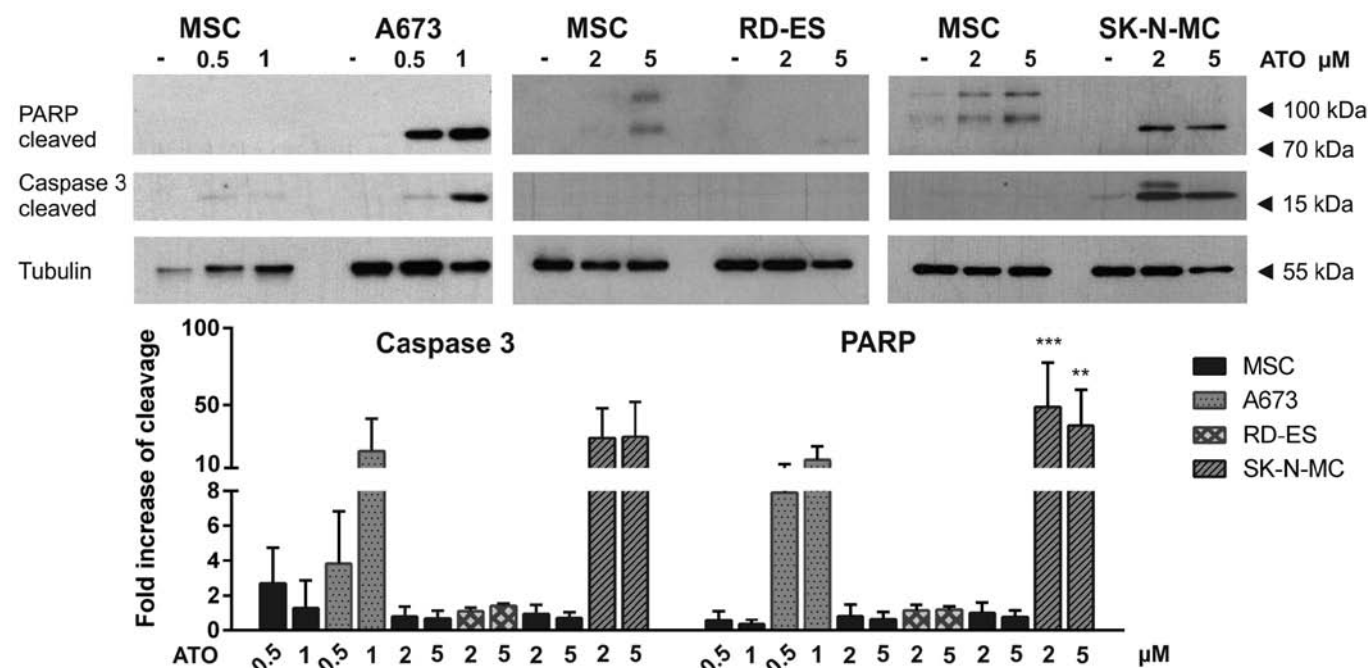

Figure 7. ATO induces apoptosis in the human ES cell lines A673 and SK-N-MC. Three ES cell lines and MSC were incubated with the ATO doses indicated for two days. Cells were lysed and subjected to western blot analysis with antibodies against cleaved PARP, cleaved caspase-3 and tubulin for loading control. Signals of three independent experiments were quantified. The graph show the mean values and standard deviations of caspase-3 and PARP cleavage (**p≤0.01, ***p≤0.001 relative to MSC PARP cleavage).

cells) as 2 μM ATO (32.1±6.3%). In SK-N-MC only the combination of 3 μM ATO and 0.5 μM etoposide induced a significantly stronger death response (34.7±4.4%) compared

to the single substances, whereas the triple combination was less efficient (27.7±7.5%). Basically, the combination of ATO and etoposide appeared to be most efficient in all ES cell
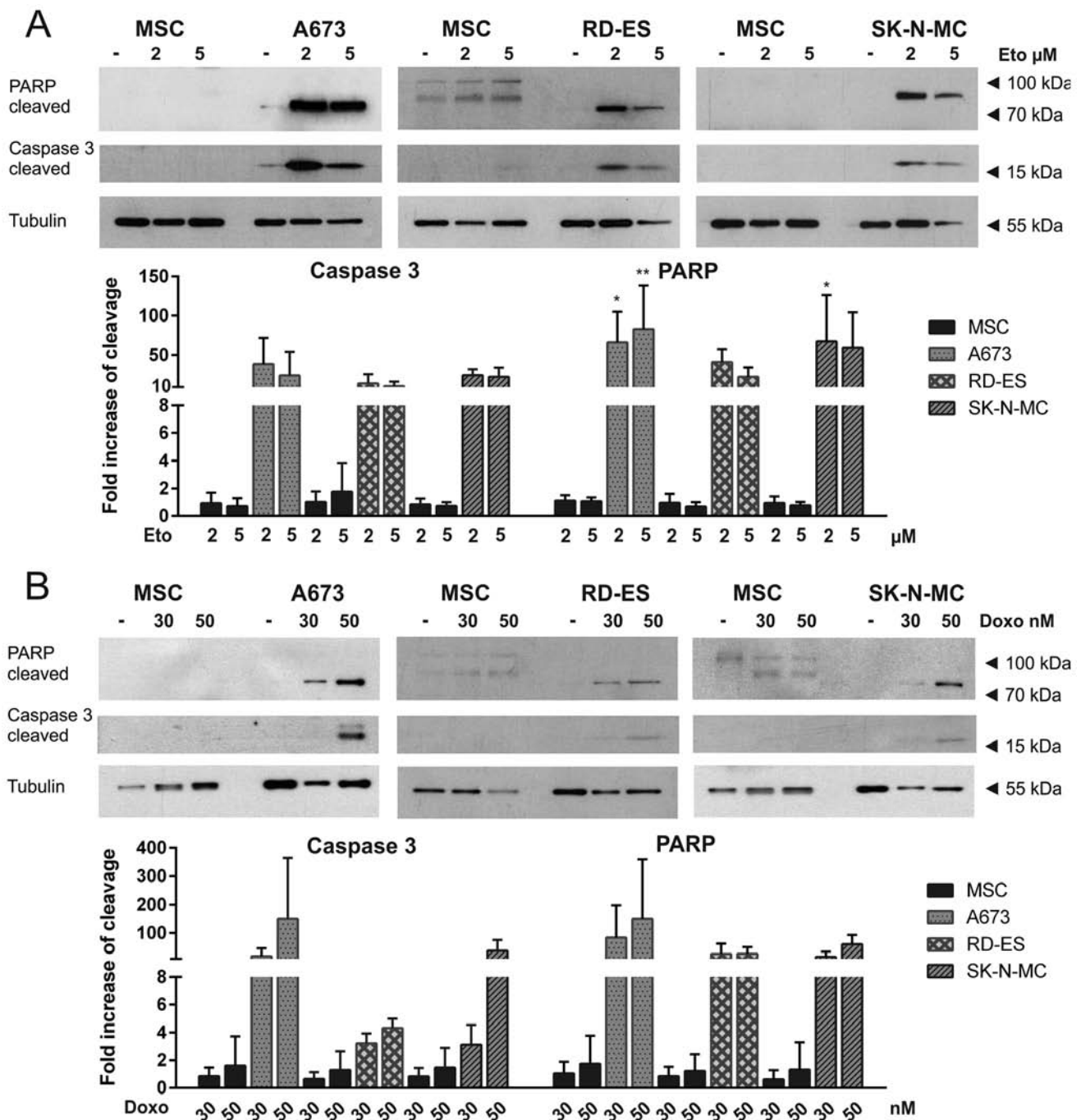
Figure 8. Etoposide and doxorubicin induce apoptosis in human ES cell lines. Three ES cell lines and MSC were incubated with: (A) etoposide (Eto) or (B) doxorubicin (Doxo) doses indicated for two days. Cells were lysed and subjected to western blot analysis with antibodies against cleaved PARP, cleaved caspase-3 and tubulin for loading control. Signals of three independent experiments were quantified. The graphs show the mean values and standard deviations of caspase-3 and PARP cleavage (*p≤0.05, **p≤0.01 relative to MSC PARP cleavage).

lines and, with the exception of A673 cells, clearly superior compared to both single applications.

ATO, etoposide and doxorubicin induce apoptosis in ES cell lines. To distinguish apoptotic from necrotic cell death, western blot analysis was performed in the three ES cell lines compared to MSC, detecting apoptotic PARP cleavage, as indicated by an 89-kDa fragment and caspase-3 cleavage represented by a l7-kDa fragment (Figs. 7 and 8). ATO induced dose-dependent apoptosis in A673 cells. Also in

SK-N-MC cells, both PARP and caspase-3 were cleaved after ATO incubation. Interestingly, in RD-ES cells neither PARP cleavage nor caspase-3 cleavage could be detected, indicating ATO induced cell death in these cells to be dependent on another mechanism (Fig. 7). Both cytostatics etoposide and doxorubicin induced apoptosis in all three ES cell lines as demonstrated by PARP and caspase-3 cleavage (Fig. 8). After long exposure of the western blots higher molecular weight PARP bands could be detected in MSC, whereas obvious caspase-3 cleavage was not observed in MSC.

Discussion

Despite initial chemo-responsiveness of primary ES, chemoresistance is observed in most patients with metastases at the time of diagnosis or upon relapse. Even using an intensive combination of vincristine, ifosfamide, doxorubicin and etoposide (VIDE), ES patients with metastatic high-risk disease expect event-free survival rates of only 20-30% (1). Drug resistance often emerges upon first line chemotherapy selecting adapted tumour cells in the whole tumour population (8). Therefore, innovative therapeutic strategies combining established chemotherapeutics with new targeted therapies are urgently needed. In this study we demonstrate that a combination of ATO with etoposide efficiently and selectively suppressed viability and colony formation accompanied by cell death induction in the EWS-FLI1 expressing ES cell lines A673, RD-ES and SK-N-MC representing three different subtypes (extraosseous, osseous and Askin's tumour = peripheral PNET, respectively) of the ES family of tumours.

Aberrant activation of the Hh signalling pathway has been found in several cancers including ES (12,20,21). However, in ES the Hh pathway is activated downstream of PTCH1 or SMO via EWS-FLI1 dependent GLI1 transcription. For this reason, SMO inhibitors are not beneficial in ES (3,12), although expression of SMO mRNA could be validated for A673, RD-ES and SK-N-MC cells. Interestingly, we found the GLI1 protein expression to be slightly lower in the ES cell lines examined compared to MSC, which are widely believed to be the cells of ES origin (22,23). The strong GLI1 mRNA expression observed in A673 cells could not be confirmed at the protein level indicating regulatory mechanisms restricting GLI1 protein translation or stability. The second activating transcription factor of the Hh pathway, GLI2, is regulated independently of EWS-FLI1 and is also no direct target of the Hh pathway itself (24). Although GLI2 mRNA expression of ES cells was similar or, in case of A673 cells, slightly elevated compared to MSC, GLI2 full length and repressor protein expression appeared to be extremely low in relation to MSC, indicating proliferation and viability of the ES cell lines A673, RD-ES and SK-N-MC to be rather dependent on GLI1 than GLI2 activity.

ATO is an FDA approved drug for treatment of acute promyelocytic leukaemia (APL) (25) and has been shown to bind both GLI1 and GLI2, thus inhibiting transactivation of their target genes and inducing GLI degradation (26,27). Beauchamp *et al* determined IC_{50} values <1 μM for ATO in A673 cells and RD-ES using WST-1 viability assays (15). We found similar sensitivities of A673 and RD-ES cells in the MTS assays. Particularly, all ES cell lines examined, including SK-N-MC, were significantly more sensitive to ATO compared to MSC, showing the high specificity of this drug, which we could also demonstrate for RMS cells in comparison to primary skeletal muscle cells (SKMC) (14). ATO plasma levels obtained in leukaemia patients are 2-5 μM, indicating clinically achievable concentrations in our experiments (28). A direct effect of ATO on EWS-FLI1 protein abundance in A673 and RD-ES cells has been excluded previously (16,29). However, in addition to targeting GLI transcription factors, cytotoxic effects of ATO also include oxidative stress and DNA damage (30,31).

GANT61, a second GLI inhibitor, also compromised MSC viability at doses below the half maximal inhibitory concentration determined for RD-ES and SK-N-MC, whereas cell death, assessed by eFluor® 450 incorporation, was neither induced in the ES cell lines nor in MSC using 15 μM GANT61. In contrast to the study of Matsumoto *et al*, we found SK-N-MC metabolic activity to be largely unaffected by GANT61 concentrations <30 μM. Moreover, cell death of the ES cell line SK-N-LO after treatment with 30 μM GANT61 appeared to be rather dependent on GLI2 inhibition, while GLI1 protein expression was hardly detectable in these cells (17). Therefore, ATO was selected for all combination experiments with etoposide and doxorubicin performed in this study.

Multidrug resistance of tumour cells emerges upon different cellular events promoting the efflux of cytostatic drugs, increasing detoxification, enhancing repair of DNA damage or impeding apoptosis (32,33). The multidrug transporter MRP1 and MDR1 are transcriptionally regulated by GLI1 (34). Especially MRP1 expression is known to be abundant in ES (9) and we could confirm its mRNA expression in all three ES cell lines examined (data not shown). Therefore, ATO might also reduce MRP1 expression augmenting the cytotoxic effects of the MRP1 substrates etoposide and doxorubicin. Apart from that, arsenic-GSH conjugates are substrates of MRP1 themselves, so that MRP1 might be additionally involved in ATO resistance (35). Moreover, in MG63 osteosarcoma cells ATO has been shown to reverse doxorubicin resistance through downregulation of stathmin expression (36). Indeed, a preliminary report of Guo *et al* mentioned the potential usefulness of ATO in combination with etoposide in Ewing sarcoma patients (37). For this reason we investigated the impact of ATO in combination with the cytostatics etoposide and doxorubicin on ES cell growth and survival.

All ES cell lines examined exhibited etoposide IC_{50} values of ~1 μM in the MTS assays. May *et al* reported clinically achievable etoposide doses of 10 μg/ml, which are clearly not obtained by our maximal applied etoposide dose of 5 μM (2.94 μg/ml) in the cell death and apoptosis assays (8). ATO in combination with etoposide significantly potentiated the viability decline and cell death induction in RD-ES and SK-N-MC cells compared to single treatments. In A673 cells, whose metabolism appeared to be extremely ATO sensitive, 0.1 μM ATO was not sufficient to augment cell death induction by 1 μM etoposide, whereas the viability was significantly reduced by the combination of these drug doses compared to single treatment. Also colony formation of A673 and RD-ES cells was clearly suppressed by the combination of ATO and etoposide compared to single application, whereas in SK-N-MC cells this effect did not become significant due to generally low colony formation rates.

RD-ES and SK-N-MC cells showed a higher resistance to doxorubicin compared to A673, determined by MTS viability assays, which was also reflected by the cell death rates obtained. This might depend on previous doxorubicin treatment of the patients as it is recorded for SK-N-MC (8). Indeed, the clinically achievable concentration of 30 ng/ml (55 nM) doxorubicin is lower than the IC_{50} values obtained for RD-ES and SK-N-MC cells (8). The combination of the ATO and doxorubicin doses applied was less effective compared to the ATO-etoposide combinations. Nevertheless, the combined

effect on viability reduction was significant in RD-ES and SK-N-MC cells, whereas colony formation was significantly compromised by the drug combination in A673 and RD-ES cells.

Application of the triple treatment consisting of ATO, etoposide and doxorubicin clearly reduced viability and induced cell death in all three ES cell lines, while MSC were not compromised by the highest concentrations used. Though, this treatment did not significantly outrank the combinations of ATO with etoposide. On the other hand, lowest colony numbers were found after the triple treatment of RD-ES and SK-N-MC.

Interestingly, RD-ES cells showed no PARP or caspase-3 cleavage upon ATO application, indicating cell death induction upon ATO in these cells to be dependent on another mechanism. Indeed, in addition to GLI inhibition, ATO has been implicated in MAPK inhibition, breakdown of mitochondrial membrane potential and ROS release leading to apoptosis, necrosis or autophagy, but also differentiation (29,38). Moreover, p53 mutations present in all ES cell lines examined, or loss of p16/p14 in A673 cells, may interfere with individual drug sensitivities (8).

This study shows, that a combination of low dose, physiologically tolerable ATO and etoposide concentrations efficiently and selectively suppressed viability and colony formation in ES cell lines, whereas cell death was enhanced. Although the exact mechanism of action of this combined effect still remains elusive, this approach appears to enhance the effectiveness of etoposide and might also prevent potential drug resistance. Moreover, adverse effects may be reduced, since individual doses can be diminished.

Acknowledgements

References

1. Jiang Y, Ludwig J and Janku F: Targeted therapies for advanced Ewing sarcoma family of tumors. Cancer Treat Rev 41: 391-400, 2015.
2. de Alava E and Gerald WL: Molecular biology of the Ewing's sarcoma/primitive neuroectodermal tumor family. J Clin Oncol 18: 204-213, 2000.
3. Cidre-Aranaz F and Alonso J: EWS/FLI1 target genes and therapeutic opportunities in Ewing sarcoma. Front Oncol 5: 162, 2015.
4. Toomey EC, Schiffman JD and Lessnick SL: Recent advances in the molecular pathogenesis of Ewing's sarcoma. Oncogene 29: 4504-4516, 2010.
5. Smith R, Owen LA, Trem DJ, Wong JS, Whangbo JS, Golub TR and Lessnick SL: Expression profiling of EWS/FLI identifies NKX2.2 as a critical target gene in Ewing's sarcoma. Cancer Cell 9: 405-416, 2006.
6. Liebner DA: The indications and efficacy of conventional chemotherapy in primary and recurrent sarcoma. J Surg Oncol 111: 622-631, 2015.
7. Paulussen M, Craft AW, Lewis I, Hackshaw A, Douglas C, Dunst J, Schuck A, Winkelmann W, Köhler G, Poremba C, et al; European Intergroup Cooperative Ewing's Sarcoma Study-92: Results of the EICESS-92 Study: Two randomized trials of Ewing's sarcoma treatment - cyclophosphamide compared with ifosfamide in standard-risk patients and assessment of benefit of etoposide added to standard treatment in high-risk patients. J Clin Oncol 26: 4385-4393, 2008.
8. May WA, Grigoryan RS, Keshelava N, Cabral DJ, Christensen LL, Jenabi J, Ji L, Triche TJ, Lawlor ER and Reynolds CP: Characterization and drug resistance patterns of Ewing's sarcoma family tumor cell lines. PLoS One 8: e80060, 2013.
9. Oda Y, Dockhorn-Dworniczak B, Jürgens H and Roessner A: Expression of multidrug resistance-associated protein gene in Ewing's sarcoma and malignant peripheral neuroectodermal tumor of bone. J Cancer Res Clin Oncol 123: 237-239, 1997.
10. Gottesman MM: Mechanisms of cancer drug resistance. Annu Rev Med 53: 615-627, 2002.
11. Beauchamp E, Bulut G, Abaan O, Chen K, Merchant A, Matsui W, Endo Y, Rubin JS, Toretsky J and Uren A: GLI1 is a direct transcriptional target of EWS-FLI1 oncoprotein. J Biol Chem 284: 9074-9082, 2009.
12. Joo J, Christensen L, Warner K, States L, Kang HG, Vo K, Lawlor ER and May WA: GLI1 is a central mediator of EWS/FLI1 signaling in Ewing tumors. PLoS One 4: e7608, 2009.
13. Zwerner JP, Joo J, Warner KL, Christensen L, Hu-Lieskovan S, Triche TJ and May WA: The EWS/FLI1 oncogenic transcription factor deregulates GLI1. Oncogene 27: 3282-3291, 2008.
14. Boehme KA, Zaborski JJ, Riester R, Schweiss SK, Hopp U, Traub F, Kluba T, Handgretinger R and Schleicher SB: Targeting hedgehog signalling by arsenic trioxide reduces cell growth and induces apoptosis in rhabdomyosarcoma. Int J Oncol 48: 801-812, 2016.
15. Beauchamp EM, Ringer L, Bulut G, Sajwan KP, Hall MD, Lee YC, Peaceman D, Ozdemirli M, Rodriguez O, Macdonald TJ, et al: Arsenic trioxide inhibits human cancer cell growth and tumor development in mice by blocking Hedgehog/GLI pathway. J Clin Invest 121: 148-160, 2011.
16. Zhang S, Guo W, Ren TT, Lu XC, Tang GQ and Zhao FL: Arsenic trioxide inhibits Ewing's sarcoma cell invasiveness by targeting p38(MAPK) and c-Jun N-terminal kinase. Anticancer Drugs 23: 108-118, 2012.
17. Matsumoto T, Tabata K and Suzuki T: The GANT61, a GLI inhibitor, induces caspase-independent apoptosis of SK-N-LO cells. Biol Pharm Bull 37: 633-641, 2014.
18. Battula VL, Treml S, Bareiss PM, Gieseke F, Roelofs H, de Zwart P, Müller I, Schewe B, Skutella T, Fibbe WE, et al: Isolation of functionally distinct mesenchymal stem cell subsets using antibodies against CD56, CD271, and mesenchymal stem cell antigen-1. Haematologica 94: 173-184, 2009.
19. Laurendeau I, Ferrer M, Garrido D, D'Haene N, Ciavarelli P, Basso A, Vidaud M, Bieche I, Salmon I and Szijan I: Gene expression profiling of the hedgehog signaling pathway in human meningiomas. Mol Med 16: 262-270, 2010.
20. Kelleher FC, Cain JE, Healy JM, Watkins DN and Thomas DM: Prevailing importance of the hedgehog signaling pathway and the potential for treatment advancement in sarcoma. Pharmacol Ther 136: 153-168, 2012.
21. Amakye D, Jagani Z and Dorsch M: Unraveling the therapeutic potential of the Hedgehog pathway in cancer. Nat Med 19: 1410-1422, 2013.
22. Lin PP, Wang Y and Lozano G: Mesenchymal stem cells and the origin of Ewing's sarcoma. Sarcoma 2011: 276463, 2011.
23. Sand LG, Szuhai K and Hogendoorn PC: Sequencing overview of Ewing sarcoma: A journey across genomic, epigenomic and transcriptomic landscapes. Int J Mol Sci 16: 16176-16215, 2015.
24. Aberger F and Ruiz I Altaba A: Context-dependent signal integration by the GLI code: The oncogenic load, pathways, modifiers and implications for cancer therapy. Semin Cell Dev Biol 33: 93-104, 2014.
25. Watts JM and Tallman MS: Acute promyelocytic leukemia: What is the new standard of care? Blood Rev 28: 205-212, 2014.
26. Raju GP: Arsenic: A potentially useful poison for Hedgehog-driven cancers. J Clin Invest 121: 14-16, 2011.
27. Kim J, Aftab BT, Tang JY, Kim D, Lee AH, Rezaee M, Kim J, Chen B, King EM, Borodovsky A, et al: Itraconazole and arsenic trioxide inhibit Hedgehog pathway activation and tumor growth associated with acquired resistance to smoothened antagonists. Cancer Cell 23: 23-34, 2013.
28. Au WY, Tam S, Fong BM and Kwong YL: Determinants of cerebrospinal fluid arsenic concentration in patients with acute promyelocytic leukemia on oral arsenic trioxide therapy. Blood 112: 3587-3590, 2008.
29. Mathieu J and Besançon F: Clinically tolerable concentrations of arsenic trioxide induce p53-independent cell death and repress NF-kappa B activation in Ewing sarcoma cells. Int J Cancer 119: 1723-1727, 2006.

30. Emadi A and Gore SD: Arsenic trioxide - An old drug rediscovered. Blood Rev 24: 191-199, 2010.
31. Sordet O, Liao Z, Liu H, Antony S, Stevens EV, Kohlhagen G, Fu H and Pommier Y: Topoisomerase I-DNA complexes contribute to arsenic trioxide-induced apoptosis. J Biol Chem 279: 33968-33975, 2004.
32. Tan B, Piwnica-Worms D and Ratner L: Multidrug resistance transporters and modulation. Curr Opin Oncol 12: 450-458, 2000.
33. Melguizo C, Prados J, Rama AR, Ortiz R, Álvarez PJ, Fernández JE and Aranega A: Multidrug resistance and rhabdomyosarcoma (Review). Oncol Rep 26: 755-761, 2011.
34. Santisteban M: ABC transporters as molecular effectors of pancreatic oncogenic pathways: The Hedgehog-GLI model. J Gastrointest Cancer 41: 153-158, 2010.
35. Leslie EM, Haimeur A and Waalkes MP: Arsenic transport by the human multidrug resistance protein 1 (MRP1/ABCC1). Evidence that a tri-glutathione conjugate is required. J Biol Chem 279: 32700-32708, 2004.
36. Feng T, Qiao G, Feng L, Qi W, Huang Y, Yao Y and Shen Z: Stathmin is key in reversion of doxorubicin resistance by arsenic trioxide in osteosarcoma cells. Mol Med Rep 10: 2985-2992, 2014.
37. Guo W, Tang XD, Tang S and Yang Y: Preliminary report of combination chemotherapy including Arsenic trioxide for stage III osteosarcoma and Ewing sarcoma. Zhonghua Wai Ke Za Zhi 44: 805-808, 2006 (In Chinese).
38. Zhao YY, Yu L, Liu BL, He XJ and Zhang BY: Downregulation of P-gp, Ras and p-ERK1/2 contributes to the arsenic trioxide-induced reduction in drug resistance towards doxorubicin in gastric cancer cell lines. Mol Med Rep 12: 7335-7343, 2015.